On the minimum thickness of doped Electron/Hole Transport Layers in organic semiconductor devices

D. Oussalah, R. Clerc, J. Baylet, R. Paquet, C. Sésé, C. Laugier, B. Racine, J. Vaillant

On the minimum thickness of doped Electron/Hole Transport Layers in organic semiconductor devices

D. Oussalah[1,2], R. Clerc[2], J. Baylet[1], R. Paquet[1], C. Sésé[1], C. Laugier[1], B. Racine[1], J. Vaillant[1].

(1) Univ Grenoble Alpes, CEA, Leti, Grenoble,38000, France
(2) Univ. Lyon, UJM-Saint-Etienne, CNRS, IOGS, Lab. Hubert Curien UMR5516, St-Etienne, France

raphael.clerc@institutoptique.fr

Abstract.

Doped hole (resp. electron) transport layers HTL (resp. ETL) are commonly used in evaporated organic devices to achieve high work function hole contact (resp. low work function electron contact) in OLED to inject large current, in solar cell to increase the open circuit voltage, and in photodetector to minimize the dark current. However, the optimisation of the HTL thickness results from a delicate trade off. Indeed, on one hand, to minimize the impact of HTL on light propagation and series resistance effects, it is commonly admitted that HTL must be kept as thin as possible. On the other hand, as discussed in this paper, due to field effect, a minimum thickness is needed to reach an efficient work function by doping. Combining modelling, simulation and experiments (performed on a template P_only TiN/STTB:F_4TCNQ/ZnPc:C_{60}/Ag device), the aim of this paper is to identify the mechanisms that determine the value of this minimum thickness.

I Introduction.

Molecular doping in organic small-molecules and polymers plays an important role in the improvement of light-emitting diodes (OLEDs)[1], solar cells[2] and photo-detector performances[3].

Indeed, in the last decades, several studies have demonstrated that increasing the number of free hole (resp. electron) concentration in organic small-molecule layer by doping was successful not only in controlling the electrical conductivity, but also its work function, as confirmed by Kelvin Probe Microscopy (KPFM) experiments[4] for instance.

This technic has been successfully used to design efficient "hole (resp. electron) transport layer", used in OLED to enhance the injected current[1], in solar cell to increase the open circuit voltage[5] and in photodetector to minimize the dark current[6]. In organic transistor, doping has been used to control the threshold voltage[7] or to improve the source and drain contacts[8].

As in inorganic semi-conductors, the doping process consists in incorporating impurities within a semiconductor matrix. In the case of organic small molecules, this process is typically done during the step of vapour deposition.

However, most of the previous studies have confirmed that the molecular doping process was less efficient than expected, and several reasons have been evoked: saturation of the effective doping and the conductivity regarding the molecular ration (MR)[9], temperature dependence of the doping efficiency[10], de-doping by the presence of traps[11], dopant diffusion[12] … It has also been reported that the efficiency of molecular doping may be less efficient when performed on ultra-thin organic layer (5 – 20 nm) compared to bulk material, which is typically the range of thickness targeted for Hole (resp. Electron) Transport Layer (HTL, resp. ETL) application[13].

The aim of this paper is to investigate in more details one of the reasons that may explain the thickness dependency of the doping efficiency in ultra-thin ETL and HTL layer: the field effect. Indeed, for a given doping, the Fermi level in ultra-thin layer may be significantly different than expected in bulk material due to the space charge effects induced by the work functions of the surrounding layers. To the best of our knowledge, this phenomenon has been less investigated in the literature so far.

To this aim, we realised samples featuring an ultra-thin 2,2',7,7'-Tetra(N,N-di-p-tolyl) amino-9,9-spirobifluorene (STTB) doped with 2,3,5,6-tetrafluoro-tetracyanoquino-dimethane (F_4TCNQ) of various molecular ratio (0% and 2%) and sandwiched between two metal contacts (Ag and TiN) and integrated in a p-only photo-diode. Electrical experiments were performed on these devices, using an original method to extract the HTL work function. Experimental results were benchmarked with simulations and interpreted using an original analytical model.

The paper is organized as follow: the fundamental question of work function control by doping in ultra-thin layer is addressed first by modelling in section II. Experiments on P only device are then presented in section III and compared with modelling, proposing an original method to extract the HTL work function. Finally, results are extrapolated on a more realistic structure by simulation, featuring both ETL and HTL.

II Modelling the work function of a thin hole transport layer.

In this section, an analytical model is derived to analyse the impact of field effect on the work function of thin HTL or ETL. The case of a semiconductor sandwiched between two metals is considered first, then

generalized to undoped semiconductor in contact with a doped HTL or ETL.

2.1 Metal /doped Semiconductor /Metal case.

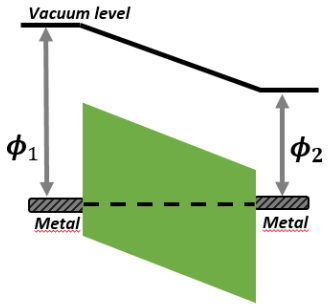

Figure 1 Band diagram of an organic semiconductor sandwiched between two metals (ϕ_1 and ϕ_2).

When a doped semiconductor is sandwiched between two metals with different work functions ϕ_1 and ϕ_2 (Figure 1), the hole concentration is no longer uniform across the semiconductor, and impacted by the presence of surrounding metals. In other words, the hole concentration results from a trade-off between the built-in field induced by the difference of work functions, and the field induced by ionized dopants. The aim of this section is to propose an analytical model to calculate the work function Φ_{HTL} resulting from this trade-off, and to investigate its dependency to the thickness of the doped organic layer.

The determination of the hole concentration, and corresponding work function Φ_{HTL} requires to solve the Poisson equation, in absence of external applied voltage, given by:

$$\frac{d^2V}{dx^2} = -\frac{e}{\varepsilon_s}\left(p_0 \exp\left(-\frac{eV}{kT}\right) - N_a\right) \quad (1)$$

where V is the electrostatic potential, N_a the hole doping concentration, e the electron charge, ε_s the semiconductor dielectric constant, T the temperature and K the Boltzman constant. $V(0) = 0$ is chosen as the boundary condition at the first metal (ϕ_1) interface, while boundary condition at the right interface becomes $V(L) = \Delta V = (\phi_1 - \phi_2)/e$, and p_0 is the hole concentration at the left metal/semiconductor interface, given by (Schottky boundary conditions):

$$p_0 = N_v \exp\left(\frac{E_g + \chi - \phi_1}{kT}\right) \quad (2)$$

Where, χ is the semiconductor electronic affinity, E_g the semiconductor gap and N_v the density of state. Introducing the potential V_f given by:

$$V_f = \frac{kT}{e} ln\left(\frac{p_0}{N_a}\right) \quad (3)$$

The Poisson equation can be re-arranged as:

$$\frac{d^2V}{dx^2} = -\frac{e}{\varepsilon_s}N_a\left(\exp\left(-\frac{e(V - V_f)}{kT}\right) - 1\right) \quad (4)$$

Such equation can be solved numerically by using Fluxim-Setfos software[14], which solves the drift diffusion equations, or analytically by performing a double integration. Example of numerical results will be given later on. However, none of these approaches allow to derive a closed form equation of the effective work function. For this reason, an approximated procedure is presented in the following. First of all, let's recall that the Poisson equation (4) can be linearized in the case of weak potential $V - V_f \ll kT/e$, becoming:

$$\frac{d^2V}{dx^2} = \frac{V - V_f}{{L_d}^2} \quad (5)$$

where L_d is the Debye length:

$$L_d = \sqrt{\frac{\varepsilon_s kT}{e^2 N_a}} \quad (6)$$

The solution of the linearized Poisson equation satisfying to the boundary conditions is:

$$V(x) = V_f\left[1 - \cosh\left(\frac{x}{L_d}\right)\right] + \left[\Delta V - V_f\left(1 - \cosh\left(\frac{L}{L_d}\right)\right)\right]\frac{\sinh\left(\frac{x}{L_d}\right)}{\sinh\left(\frac{L}{L_d}\right)} \quad (7)$$

However, as ΔV is typically much larger than kT/e in practical cases, the following approximation does not reproduce the simulations. For this reason, the proposed model consists in using the same equation that meet the boundary conditions, replacing the Debye length L_d by an effective length L*. The parameter L* can be determined by the following procedure. Indeed, according the Poisson equation (5), this distance should satisfy the following equation:

$$\frac{d^2V}{dx^2} = \frac{V(x, L^*) - V_f}{{L^*}^2} = -\frac{e}{\varepsilon_s}N_a\left(\exp\left(-\frac{e(V(x, L^*) - V_f)}{kT}\right) - 1\right) \quad (8)$$

Taking the spatial average of the previous equation, L* is found numerically as a solution of the following transcendental equation:

$$\int_0^L \left[\frac{V(x, L^*) - V_f}{{L^*}^2} + \frac{e}{\varepsilon_s}N_a\left(\exp\left(-\frac{e(V(x, L^*) - V_f)}{kT}\right) - 1\right)\right]dx = 0 \quad (9)$$

The numerical solution (called "simulation") of equation (1) obtained using a drift diffusion solver and the approximated model of equation (7) are plotted in Figure 2 for different HTL thicknesses and a volume doping level equal to 2.10^{18} cm^{-3}. Both curves are in

good agreement. Our model efficiently captures the charge re-arrangement due to the combined effects of doping and surrounding work functions.

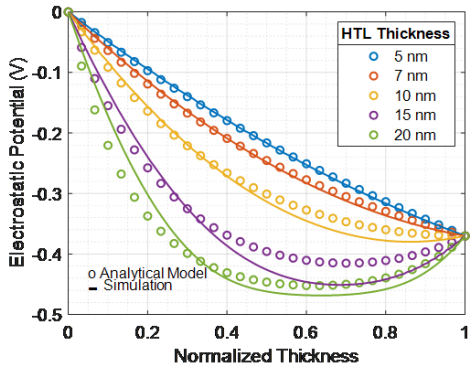

Figure 2 : Electrostatic potential in a doped organic semi-conductor (N_a =2.10^{18} cm^{-3}, homo=-5.25 eV and lumo=-4.5 eV) sandwiched between two metals of work functions ϕ_1=-4.7 eV and ϕ_2=-5.05 eV.

In particular, it can be seen that the potential within the semiconductor is never flat, as it would be expected in a bulk, thick layer. In this example, the minimum thickness required to efficently tune the semiconductor work function by doping and make it play the role of an efficient hole transport layer should be equal or larger than 20 nm (Figure 3).

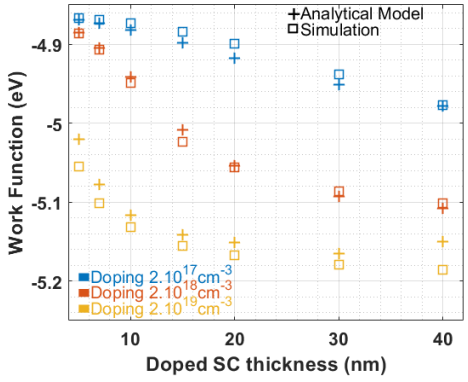

Figure 3. Effective work function in a doped organic semi-conductor (N_a =2.10^{17} cm^{-3}: blue marks and N_a =2.10^{18} cm^{-3}: red marks, N_a =2.10^{19} cm^{-3}: yellow marks, homo=-5.25 eV and lumo=-4.5 eV) sandwiched between two metals of work functions ϕ_1=-4.7 eV and ϕ_2=-5.05 eV.

Moreover, as the potential is not constant, it is not easy to define accurately the notion of work function within the semiconductor layer. To give a number, we introduce the notion of "effective" work function, calculated by taking once again the spatial average :

$$W_f = \phi_1 - e\int_0^L V(x,L^*)\frac{dx}{L} \qquad (10)$$

After straightforward calculations, we found that:

$$W_f = \phi_1 - eV_f - e(\Delta V - 2V_f)\frac{L^*}{L}\tanh\left(\frac{L}{2L^*}\right) \qquad (11)$$

Model (11) and numerical simulations are compared in Fig. 2, showing again an overall very good agreement.

2.2 Metal /doped Semiconductor (HTL) / undoped semiconductor /Metal case.

In pratical case however, the hole transport layer (HTL) is never sandwitched between two metals, but rather between one metal and an undoped semiconductor layer (typically a blend of a donor and acceptor molecules for solar cell device). This situation impacts the charge repartition within the HTL, as a fraction of the voltage drop due to the difference of work functions will occur in the undoped semiconductor layer. The previously presented model can be improved to account for this effect. In a Metal/doped Semiconductor (HTL)/undoped semiconductor/Metal structure, the linearized Poisson equation (5) becomes :

$$\frac{d^2V_1}{dx^2} = \frac{V_1 - V_f}{{L_d}^2} \quad for\ 0 < x < L_{HTL}$$
$$\frac{d^2V_2}{dx^2} = 0 \quad for\ L_{HTL} < x < L \qquad (12)$$

Where L_{HTL} is the thickness of the HTL layer. Boundary conditions remains unchanged at x = 0 and x = L, but solutions have to be matched at x = L_{HTL}, according the following standard procedure :

$$V(L_{HTL}^-) = V(L_{HTL}^+) \qquad (13)$$

$$\varepsilon_{s1}\frac{dV_1}{dx}(L_{HTL}^-) = \varepsilon_{s2}\frac{dV_2}{dx}(L_{HTL}^+) \qquad (14)$$

Numerical and analytical solutions are compared in Fig. 3. The overall agreement is not as good as previously, especially in the undoped semiconductor, when thicker HTL layers are considered. Indeed, equation (12) assumes that there is stricly no charge inside the undoped layer, which is not exactly the case, as free hole may diffuse through the undoped semiconductor. However, as the trend of the electrostatic potential inside the HTL layer (where the effective work function is calculated) remains acceptable in all cases (see Fig. 4), we did not try to improve further the model to include the impact of hole diffusion within the undoped layer. As seen in Fig. 4, the effective work function calculed using eq. (10), (replacing L by L_{HTL}), correctly reproduced numerical simulations.

$$W_f = \phi_1 - eV_f - \frac{e}{\delta}\frac{(\Delta V - 2V_f)\tanh(\delta/2) - V_f(\gamma - \delta)}{1 + (\gamma - \delta)\ \coth(\delta)} \qquad (15)$$

With: $\delta = \frac{L_{HTL}}{L^*}$ and $\gamma = \frac{L}{L^*}$

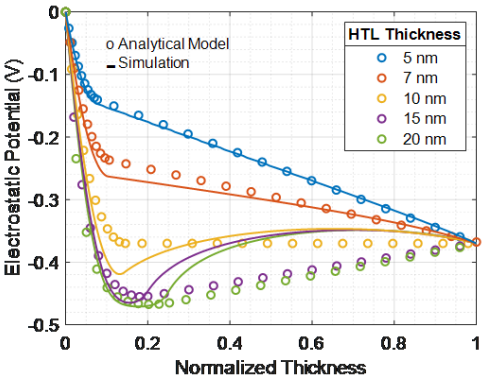

Figure 4. Electrostatic potential at 0 V in a doped organic semi-conductor (N_a =2.10^{18} cm^{-3}, Homo=-5.25 eV and Lumo=-4.5 eV) sandwiched between a metal and an undoped semiconductor (60 nm). Metal work functions are ϕ_1=- 4.7 eV and ϕ_2=-5.05 eV.

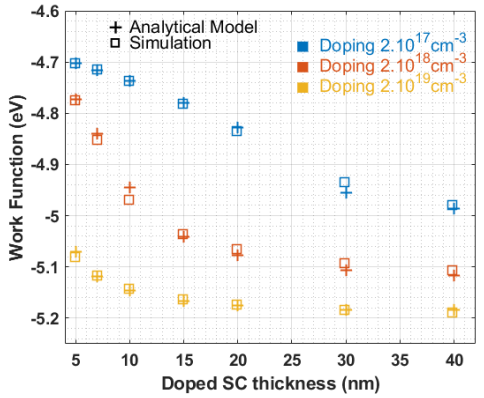

Figure 5 : Effective work function in a doped organic semi-conductor (N_a =2.10^{17} cm^{-3}: blue marks and N_a =2.10^{18} cm^{-3}: red marks, N_a =2.10^{19} cm^{-3}: yellow marks, Homo=-5.25 eV and Lumo=-4.5 eV) sandwiched between a metal and an undoped semiconductor (60 nm). Metal work functions are ϕ_1=- 4.7 eV and ϕ_2=-5.05 eV.

Interesingly, the presence of an undoped layer has a positive impact on the HTL effective work function. Indeed, by comparing Fig. 2 and Fig. 4, it appears that a HTL thickness of 15nm (rather then 20nm) and, 10nm (rather then 15nm) may be acceptable for a p-doping concentration of 2.10^{18} cm^{-3} and 2.10^{19} cm^{-3} respectively, to reach the lowest work function possible. This can be understood as follow : in Metal/doped Semiconductor (HTL)/ undoped semiconductor/Metal stack, thanks to the voltage drop in the undoped layer, the difference of potential seen by the HTL is reduced, and in consequence, it is easier for the doped layer to reach equilibrium.

Before discussing in more details the required thickness for achieving lowest HTL (and ETL) work functions, experiments have been performed in a simplified organic photodiode (OPD) device, to validate the modelisation.

III Comparison with experiments

3.1 Device processing.

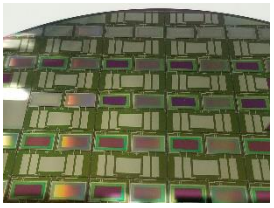

Figure 6 : Image of a top view of the 200 mm silicon wafer processed to realize TiN/ STTB:F_4TCNQ /ZnPc:C_{60} /Ag devices.

In this section, the main process steps of device fabrication are summarized. The molecules (Zinc phtalocyanine (ZnPc), Fullerene-C_{60} (C_{60}), STTB and F_4TCNQ) used in this study were purchased from Sigma Aldrich. Devices were fabricated using a cleaned 200 mm patterned silicon substrate wafer (see Figure 6) with an Al-Cu/TiN as bottom electrode. The different layers were deposited by thermal evaporation in a vacuum chamber. The devices discussed in this paper have the following structure: TiN /ZnPc:C_{60}/ STTB:F_4TCNQ/ Ag (see a schematic band diagram on Figure 7). This stack does not correspond to a classical stack for OLED or PV devices, in particular because it does not include an ETL contact. This has been done on purpose, to extract the HTL work function more easily, avoiding uncertainty induced by the use of a doped ETL. To prevent from degradation due to oxygen exposure, devices were encapsulated with 25nm of SiO, followed by 25nm of Al_2O_3. TiN and Ag are used as the contact electrodes and their work function are measured by KPFM. ZnPc:C_{60} represents the active layer. STTB:F_4TCNQ is the studied doped HTL layer. Hence, STTB doped F4TCNQ at ratios of 0% (undoped) and 2% with 5 nm, 10 nm and 15 nm of thicknesses were processed.

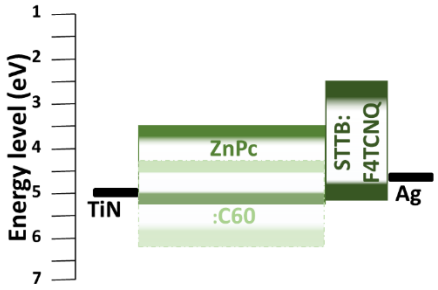

Figure 7 : Schematic energy-level diagram the OPD structure. TiN and Ag work function were measured using KPFM. Energy levels of ZnPc, C60 and F4TCNQ were taken from literature [15]

3.2 Work function extraction procedure.

As the HTL are integrated in stacked OPDs and sensible to air exposure, it is not possible to perform direct work function measurement by classical method such as KPFM and ultraviolet Photoelectron Spectroscopy (UPS). In this paper, an alternative technics is proposed, following the work of X. Wei et. al.[16]. This extraction is based on the fact that, in first order approximation, all I-V curves under illumination intercept at the same point, for voltage V_{cross} equal to:

$$V_{cross} = \phi_2 - \phi_1 = -V_{bi} \quad (15)$$

An example is shown in Figure 8.

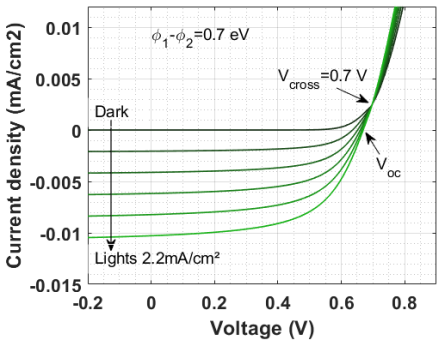

Figure 8 : Illustration of the work function extraction procedure by a simulated I-V curve of ZnPc:C60 sandwiched between two metals. All the illuminated I-V curves intercept at the same voltage V_{cross}. In this example, $V_{cross} = \phi_2 - \phi_1 = 0.7$ *V.*

This assumption has been investigated further by the mean of drift diffusion simulations in a simplified Metal/Semiconductor/Metal architecture, where the contact work functions were artificially tuned (from 0.2 to 0.8 eV). Results shown in Figure 9 confirms that V_{cross} is indeed equal to the difference of work function Eq. (15).

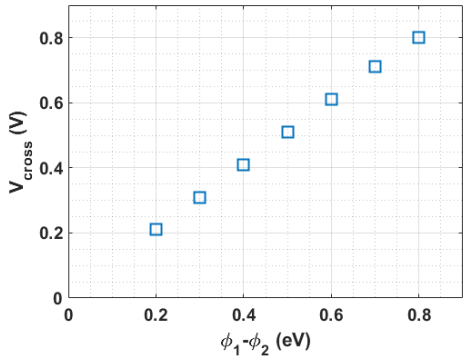

Figure 9 : Simulation of the potential V_{cross} *(voltage where all the I-V characteristics under different light irradiances intercept) versus metal work function difference* $(\phi_2 - \phi_1)$. *The simulation was performed on the OPD structure of TiN/ZnPc:C60/Ag.*

In the case where a doped HTL is stacked between the metal contact (ϕ_2) and the undoped semiconductor layer (see Figure 10), the voltage V_{cross} is no longer controlled by the two contact metals as expected, but by the metal (ϕ_1) and the work function of the doped HTL (ϕ_{HTL}). Thus, V_{cross} becomes:

$$V_{cross} = \phi_{HTL} - \phi_1 \quad (16)$$

By measuring V_{cross} and knowing ϕ_1, ϕ_{HTL} is deducted using the previous equation:

$$\Phi_{HTL} = \phi_1 - V_{cross} \quad (17)$$

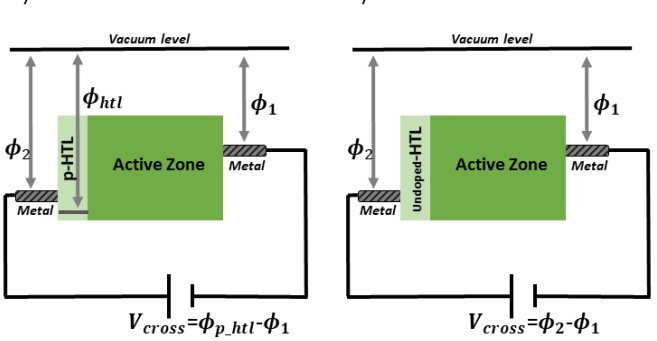

Figure 10. Band diagram of metal/p-doped HTL (a) and undoped HTL (b)/organic semiconductor/metal at V_{cross}. ϕ_1 and ϕ_2 are the metal work function.

3.3 Experimental results: I-V curves.

In this section, experimental I-V curves measured on device featuring doped and undoped STTB layers are discussed and compared with simulations.

All the experimental curves in dark and light conditions (10-100 $\mu W/cm^2$) were fitted (Figure 11) with a drift diffusion solver, using the same material parameters, reported in Table 1.

	Ag		TiN
Work Function [eV]	-4.7		-4.9
	ZnPc:C$_{60}$	STTB	STTB:F$_4$TCNQ
Homo [eV]	-5.25	-5.25	-5.25
Lumo [eV]	-4	-4	-4
μ [cm^2/Vs]	7.10^{-7}	10^{-3}	5.10^{-4}
Υ [$\sqrt{cm/V}$]	3.10^{-3}		
ε	3.5	3.5	3.5
Doping [cm^{-3}]			2.10^{18}
Trap Density [cm^{-3}]		5.10^{17}	

Table 1. Parameters used in simulation presented in Figure 11.

The overall good agreement between simulations and experiments, using the same material parameters, confirms the capability of the simulation to reproduce electron and hole transport in these devices. Only the thicknesses and the doping levels change from one sample to another, as expected from sample

preparation. The doping level was not measured directly (it is difficult to extract the doping level on such thin STTB layers), however, a reasonable agreement between theory and experience has been found assuming N_d = 2.10^{18} cm^{-3} for STTB doped with F_4TCNQ at 2% molecular ratio. This value is same order of magnitude with data reported by K. Leo & al[17]

First of all, the I-V characteristics of the device with thickness of 5 nm and 10 nm of STTB:F_4TCNQ at 2% ratio are plotted in Figure 11-a-b respectively. For a thickness of 5 nm, all the I-V characteristics cross at one voltage of -0.09 V. On the other hand, for a thickness of 10 nm the cross voltage is at 0.06 V, in agreement with the variation of the STTB:F_4TCNQ (2%) work function. The change of sign indicates an inversion of the sign of the $\phi_{HTL} - \phi_1$, on line with theory.

Secondly, for undoped STTB, the cross voltage is approximately the same: -0.36 V and -0.39 V for a thickness of 5 nm and 10 nm respectively (Figure 11 c and d). Indeed, as the STTB is undoped, it no longer behaves as a hole injection contact. In this case, the electrode work function is fixed by the TiN metal. Thus, the hole contact work function should not be affected by the thickness of the STTB, and as expected, the I-V characteristics of the devices with 5 nm and 10 nm thickness of STTB approximately intercept at the same V_{cross}. The observed slight difference is probably due to the work function variation of TiN, known to depend to sample preparation.

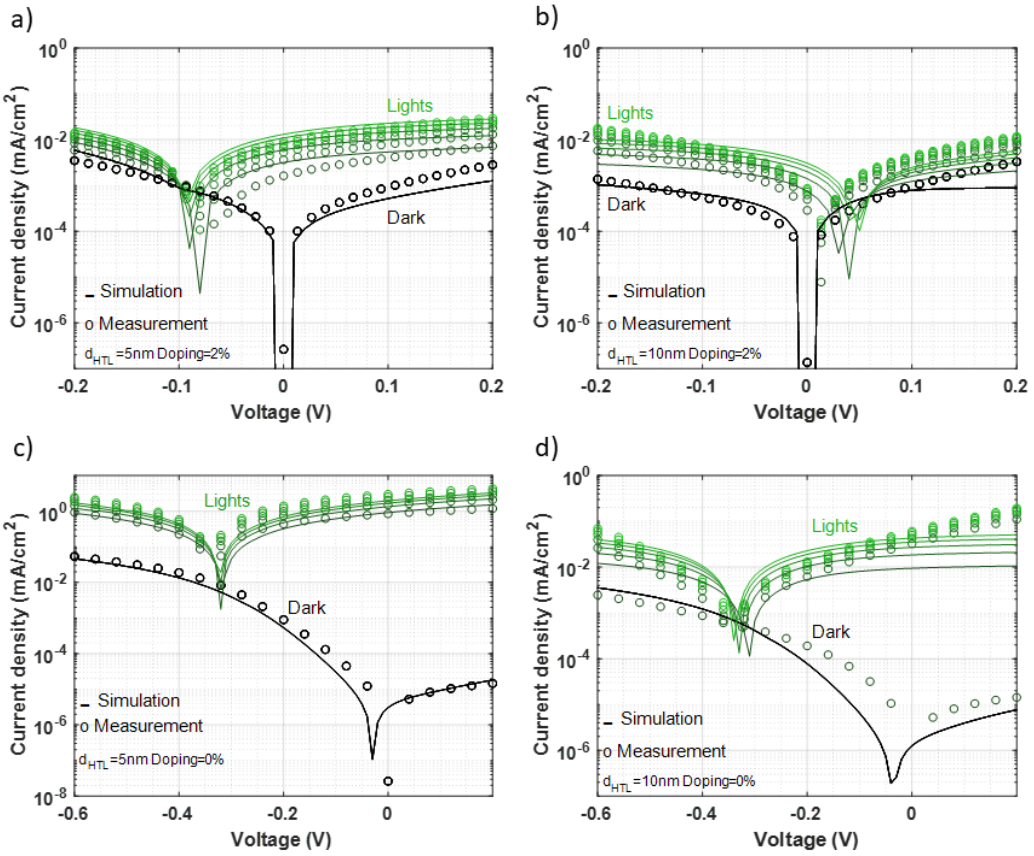

Figure 11. Dark and illuminated I-V curves. Circles are experimental datas, solid lines are simulations. STTB has been doped with F4TCNQ (2%) in Figures a) and b). In this later case, the effective doping used in the simulation is $2.10^{18}\ cm^{-3}$ *in both case. In Figures c) and d), the STTB is undoped. The STTB thickness is 5 nm in figures a) and c), and 10 nm in figures b) and d). All the others parameters are reported in Table 1.*

3.4 Experimental results: Work function.

Figure 12 shows a comparison between the numerical simulations, analytical models and measurements of the work function of the undoped STTB and doped STTB with F_4TCNQ with a 2% molar ratio. It has to be noted that the thickness of ultra-thin STTB layer is known with a $\pm$ 2 nm uncertainty, reported in Figure 12 as error bars. Similarly, the value of the measured work function has been averaged on several samples and the standard deviation has been also included as error bars.

When the HTL is undoped, the V_{cross} measured should represent simply, as previously mentioned, the work function difference between ϕ_1 and ϕ_2. Hence, I-V characteristics of the devices with *undoped* STTB thickness of 5, 10 and 15 nm intercept at the same voltage. Consequently, the work function deduced is not due to STTB in this case, but due to the Ag contact.

The results obtained are presented on the Figure 12 (blue circles), the work function measured with 5 and 10 nm of undoped STTB are in good agreement with the simulation. However, the device with 15 nm of undoped STTB slightly differs, this difference could be attributed to degradation of the reference electrode (TiN work function) due to atmosphere oxidation [18].

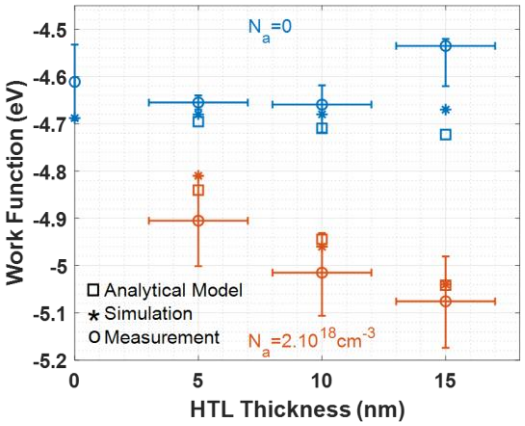

Figure 12. Work function versus thickness calculated using model, simulation or measured versus thickness of undoped HTL (blue marks) and p-doped HTL with a 2% molar ratio (red marks). The doping level in numerical and analytical calculation is $2.10^{18}\ cm^{-3}$.

In the p-doped HTL devices, the V_{cross} measured represents the work function difference between ϕ_1 and ϕ_{HTL}. As shown in Figure 11, V_{cross} measured is - 0.09 and 0.05 V for devices with 5 and 15 nm of doped HTL thickness respectively. Note that, the V_{cross} sign changing is directly related to the sign of $\phi_1 - V_{HTL}$. The red marks, represented on Figure 12, bring out the thickness dependence of a p-doped HTL work function. Indeed, the work function measured is -4.9, -5.01 and - 5.09 eV for a p-doped HTL (ratio of 2%) thickness of 5, 10 and 15 nm respectively. These results are in good agreement with the theoretical simulations and models. However, a slight difference is present for the devices with a thickness 5 and 10 nm. This disparity could be due to an error in the deposit layer thickness, as well as a variation of the doping ratio (due to the instability of the deposition rate).

Despite experiment uncertainties, these data confirm that the control of the work function in HTL by doping is thickness dependant, following the trend predicted by drift diffusion theory.

IV Minimum HTL thickness for an ideal p-i-n organic photodiode.

The p-i-n diode is the most typical structure used in OPVs/OPDs[19]. In this section, we propose to estimate the minimum thickness required to achieve an efficient p-doped HTL work function in a more realistic device architecture. To this aim, we have simulated the following typical OPD stack: metal/ p-doped HTL/intrinsic active-layer (50nm)/n-doped ETL (15nm)/metal. The HTL work function has been extracted and plotted versus thickness for different p-doping concentrations on Figure 13.

The lowest work function achievable by a p-doped HTL strongly depend on it thickness, as explained and shown above. Nevertheless, the required thickness depends additionally on the doping concentration. Indeed, as represented on Figure 13, the minimum thickness needed to reach the optimum work function is 15, 20, 25 and 30 nm for a p-doping concentration of 10^{19}, 5.10^{18}, 10^{18} and 5.10^{17} cm^{-3} respectively. Hence, for very high doping concentration (10^{19}-10^{20} cm^{-3}), a very thin thickness (10-15 nm) is enough to reach the optimum work function for a given doping concentration (as shown in Figure 13, -5.17 and -5.03 eV at a p-doping concentration of 5.10^{17} cm^{-3} and 10^{19} cm^{-3} respectively).

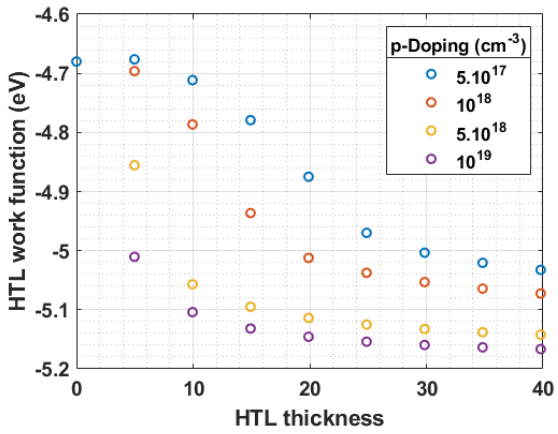

Figure 13. Simulation of the HTL work function with respect of it thickness in a p-i-n OPD structure. HTL p-doping is $5.10^{17}\ cm^{-3}$ *(blue circles),* $10^{18} cm^{-3}$ *(red circles),* $5.10^{18}\ cm^{-3}$ *(yellow circles) and* $10^{19}\ cm^{-3}$ *(purple circles).*

However, as it is difficult to achieve such level of doping in organic semiconductors[9], a higher thickness (> 20 nm) may be needed, as shown in Figure 13. As consequence, the p-doped HTL thickness should be carefully examined to obtain a higher efficient p-i-n photodetector.

V Conclusions.

This paper has investigated a limitation of work function control in doped Hole Transport Layer HTL (or by extension, Electron Transport Layer) due to field effect. Indeed, as the concentration of free carriers within the HTL is not infinite, a minimum thickness is needed in order to achieve the lowest possible work function. This effect has been highlighted by three different approaches: analytical modeling, numerical simulation, and experiments, performed on template devices featuring F_4TCNQ doped STTB HTL of different thicknesses, but no ETL (to facilitate HTL work function extraction). Despite experimental difficulties in controlling accurately the doping level and the thickness of HTL, experimental results clearly confirm the trend of the work function versus thickness predicted by the theory. At last, simulations have been performed in a more classical p-i-n organic device architecture, suggesting that the minimum thickness for a low work function HTL is around 10 nm at high doping levels ($> 10^{19}$ cm^{-3}), but can reach 20 nm at moderate doping levels (10^{18} cm^{-3}). These results constitute precious indications for the design of efficient organic LED, solar cell or photodetectors.

References:

[1] W. Zhao, Z. Shi, H. Cao, L. Chen, and D. Qin, Thin Solid Films **642**, 333 (2017).

[2] M.L. Tietze, W. Tress, S. Pfützner, C. Schünemann, L. Burtone, M. Riede, K. Leo, K. Vandewal, S. Olthof, P. Schulz, and A. Kahn, Phys. Rev. B **88**, (2013).

[3] B. Wang, A.D. Scaccabarozzi, H. Wang, M. Koizumi, M.I. Nugraha, Y. Lin, Y. Firdaus, Y. Wang, S. Lee, T. Yokota, T.D. Anthopoulos, and T. Someya, J. Mater. Chem. C **9**, 3129 (2021).

[4] H. Hoppe, T. Glatzel, M. Niggemann, A. Hinsch, M.C. Lux-Steiner, and N.S. Sariciftci, Nano Lett. **5**, 269 (2005).

[5] N. Shintaku, M. Hiramoto, and S. Izawa, J. Phys. Chem. C **122**, 5248 (2018).

[6] C.-C. Lee, S. Biring, S.-J. Ren, Y.-Z. Li, M.-Z. Li, N.R. Al Amin, and S.-W. Liu, Org. Electron. **65**, 150 (2019).

[7] Y. Abe, T. Hasegawa, Y. Takahashi, T. Yamada, and Y. Tokura, Appl. Phys. Lett. **87**, 153506 (2005).

[8] J. Li, X.-W. Zhang, L. Zhang, Khizar-ul-Haq, X.-Y. Jiang, W.-Q. Zhu, and Z.-L. Zhang, Solid State Commun. **149**, 1826 (2009).

[9] I. Salzmann, G. Heimel, M. Oehzelt, S. Winkler, and N. Koch, Acc. Chem. Res. **49**, 370 (2016).

[10] M.L. Tietze, J. Benduhn, P. Pahner, B. Nell, M. Schwarze, H. Kleemann, M. Krammer, K. Zojer, K. Vandewal, and K. Leo, Nat. Commun. **9**, (2018).

[11] M.L. Tietze, K. Leo, and B. Lüssem, Org. Electron. **14**, 2348 (2013).

[12] J. Li, C.W. Rochester, I.E. Jacobs, S. Friedrich, P. Stroeve, M. Riede, and A.J. Moulé, ACS Appl. Mater. Interfaces **7**, 28420 (2015).

[13] X. Liu, Y. Lin, Y. Liao, J. Wu, and Y. Zheng, J. Mater. Chem. C **6**, 3499 (2018).

[14]Fluxim (https://www.fluxim.com/)

[15] W. Zeng, K.S. Yong, Z.M. Kam, F. Zhu, and Y. Li, Appl. Phys. Lett. **97**, 133304 (2010).

[16] X. Wei, M. Raikh, Z.V. Vardeny, Y. Yang, and D. Moses, Phys. Rev. B **49**, 17480 (1994).

[17] S. Olthof, W. Tress, R. Meerheim, B. Lüssem, and K. Leo, J. Appl. Phys. **106**, 103711 (2009).

[18] I. Montero, C. Jimenez, and J. Perriere, Surf. Sci. **251**, 1038 (1991).

[19] B. Lüssem, M. Riede, and K. Leo, Phys. Status Solidi A **210**, 9 (2013).

Data availability:

The data that support the findings of this study are available from the corresponding author upon reasonable request.